

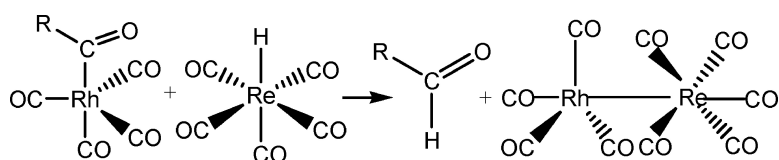
Article

Synchronicity of Mononuclear and Dinuclear Events in Homogeneous Catalysis. Hydroformylation of Cyclopentene Using Rh(CO) and HRe(CO) as Precursors

Chuanzhao Li, Li Chen, and Marc Garland

J. Am. Chem. Soc., 2007, 129 (43), 13327-13334 • DOI: 10.1021/ja073339v • Publication Date (Web): 05 October 2007

Downloaded from <http://pubs.acs.org> on February 14, 2009



More About This Article

Additional resources and features associated with this article are available within the HTML version:

- Supporting Information
- Links to the 7 articles that cite this article, as of the time of this article download
- Access to high resolution figures
- Links to articles and content related to this article
- Copyright permission to reproduce figures and/or text from this article

[View the Full Text HTML](#)



ACS Publications
 High quality. High impact.

Synchronicity of Mononuclear and Dinuclear Events in Homogeneous Catalysis. Hydroformylation of Cyclopentene Using $\text{Rh}_4(\text{CO})_{12}$ and $\text{HRe}(\text{CO})_5$ as Precursors

Chuanzhao Li,^{†,‡} Li Chen,[†] and Marc Garland^{*,†,‡}

Contribution from the Department of Chemical and Biomolecular Engineering, National University of Singapore, 117576, and Institute of Chemical and Engineering Sciences, 1 Pesek Road, Jurong Island, Singapore, 627833

Received May 11, 2007; E-mail: marc_garland@ices.a-star.edu.sg

Abstract: The combined application of two or more metals in homogeneous catalysis can lead to synergistic effects; however, the phenomenological basis for these observations often goes undetermined. The heterobimetallic catalytic binuclear elimination reaction, a system involving both mononuclear and dinuclear intermediates, has been repeatedly suggested as a possible mechanism. In the present contribution, the simultaneous application of $\text{Rh}_4(\text{CO})_{12}$ and $\text{HRe}(\text{CO})_5$ as precursors in the hydroformylation reaction leads to a very strong synergistic rate effect. In situ spectroscopic measurements confirm the presence of both mononuclear and dinuclear intermediates such as $\text{RCORh}(\text{CO})_4$ and $\text{RhRe}(\text{CO})_9$ in the active system. Moreover, kinetic analysis confirms interconversion of these intermediates as well as their statistical correlation with organic product formation. Specifically, the rate of hydrogen activation by $\text{RhRe}(\text{CO})_9$ is exactly equal to the rate of aldehyde formation from binuclear elimination between $\text{HRe}(\text{CO})_5$ and $\text{RCORh}(\text{CO})_4$ at all reaction conditions studied. Thus the catalytic events involving mononuclear species and those involving dinuclear species are synchronized. In the present experiments, the new topology is orders of magnitude more efficient than the corresponding unicyclic rhodium system.

Introduction

The catalytic hydroformylation reaction, consisting of the addition of carbon monoxide and hydrogen to alkenes to form aldehyde (and their corresponding alcohols) was discovered by Roelen in 1938.^{1,2} Today, this reaction is the fifth largest homogeneously catalyzed reaction worldwide with more than 6.6×10^6 tonnes of products produced per annum.³ Cobalt and rhodium are the principal metals used, particularly for the industrial processes. The metals are used in both their unmodified as well as phosphine modified forms.⁴ It is widely accepted that rhodium is by far the most active metal for the transformation of alkenes to aldehydes.⁵ The use of phosphine modified rhodium for the hydroformylation reaction was extensively explored with monodentate ligands in Sir Geoffrey Wilkinson's group.⁶ Since then, an enormous number of other phosphine modified rhodium systems have been developed to enhance activity and to better control regio- and stereochemical aspects, especially for fine chemicals and pharmaceuticals.⁷ In many

respects, the organorhodium precursors and chemistry used in current large-scale industrial rhodium-catalyzed hydroformylations do not significantly differ from the original patents and reports on unmodified and modified systems.⁸

The Heck–Breslow mechanism for hydroformylation, consisting of a unicyclic reaction system of mononuclear intermediates, was first proposed for the unmodified cobalt system.⁹ According to the originally proposed mechanism, the formation of a crucial mononuclear hydride species is followed by alkene coordination and π -complex formation, insertion and alkyl formation, CO insertion, oxidative addition of hydrogen, and then hydrogenolysis of the Co–C bond as shown in Scheme 1. All steps were considered reversible, with the exception of the hydrogenolysis. Subsequently, studies of high-temperature unmodified cobalt-catalyzed hydroformylation showed that the last step can be reversible.¹⁰

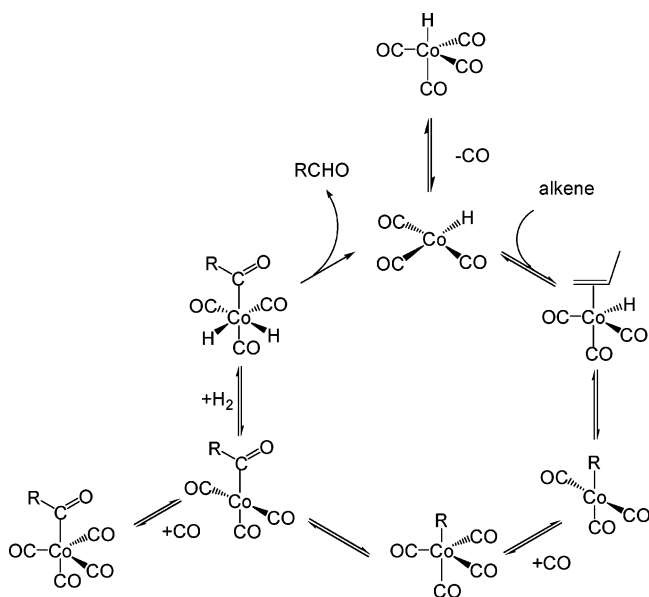
With regard to other related systems, a deuterioformylation with a bidentate phosphine-modified rhodium system at ca. 34 °C indicated very little reversibility for the initial step involving metal hydride attack on alkene,^{11a} and a bidentate phosphine-

[†] National University of Singapore.

[‡] Institute of Chemical and Engineering Sciences.

- (1) Roelen, O. U.S. Patent 2,327,066, 1943.
- (2) Falbe, J. *New Syntheses with Carbon Monoxide*; Springer: New York, 1980.
- (3) Kamer Paul, C. J.; Reek Joost, N. H.; van Leeuwen Piet, W. N. M. Rhodium Catalyzed Hydroformylation. In *Mechanisms in Homogeneous Catalysis: A Spectroscopic Approach*; Heaton, B., Ed.; Wiley: Germany, 2005; pp 231–267.
- (4) Bahrmann, H.; Bach, H. Oxo Synthesis. In *Ullmann's Encyclopedia of Industrial Chemistry*; Wiley-VCH: Germany, 2002.
- (5) Csontos, G.; Heil, B.; Marko, L. *Ann. N.Y. Acad. Sci.* **1974**, 239, 47–54.
- (6) Evans, D.; Osborn, J. A.; Wilkinson, G. J. *Chem. Soc. A* **1968**, 12, 3133–42.

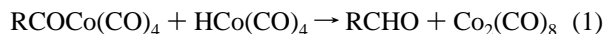
- (7) Consiglio, G.; Pino, P. *Top. Curr. Chem.* **1982**, 105, 77–123.
- (8) (a) Schiller, G. (Chem. Verwertungsges. Oberhausen) Catalyst for Oxo Synthesis. German Patent 953,605. (b) Hughes, V. L. Catalytic oxidation of olefins. U.S. Patent 2,880,241, 1959.
- (9) (a) Breslow, D. S.; Heck, R. F. *Chem. Ind. (London)* **1960**, 467. (b) Heck, R. F.; Breslow, D. S. *J. Am. Chem. Soc.* **1961**, 83, 4023–4027.
- (10) Kim, C.; Matsui, Y.; Orchin, M. *J. Organomet. Chem.* **1985**, 279, 159–164.
- (11) (a) Casey, C. P.; Petrovich, L. M. *J. Am. Chem. Soc.* **1995**, 117, 6007–14. (b) Casey, C. P.; Martins, S. C.; Fagan, M. A. *J. Am. Chem. Soc.* **2004**, 126, 5585–5592.

Scheme 1. Heck–Breslow Cobalt-Catalyzed Hydroformylation Mechanism

modified Pt–Sn hydroformylation system indicated that the last step (hydrogenolysis) was essentially irreversible at 39 °C and but reversible at 98 °C.^{11b}

A similar Heck–Breslow type mechanism was then proposed for the unmodified rhodium-catalyzed hydroformylation¹² and the modified rhodium-catalyzed hydroformylation.¹³ In the past two decades, with the increased use of in situ spectroscopic studies, both rhodium tetracarbonyl hydride $\text{HRh}(\text{CO})_4$ ¹⁴ and acyl rhodium tetracarbonyl $\text{RCORh}(\text{CO})_4$ have been observed for unmodified rhodium systems.¹⁵ Detailed kinetic modeling has repeatedly shown that the hydrogenolysis of the Rh–C bond in $\text{RCORh}(\text{CO})_4$ is the rate-limiting step.¹⁶ These latter findings are consistent with a unicyclic reaction mechanism, where all intermediates are unmodified *mononuclear* rhodium complexes.

A second, significantly different mechanism was also proposed by Heck and Breslow for the cobalt-catalyzed hydroformylation.⁹ This second mechanism consists of the simultaneous presence of both mononuclear and dinuclear intermediates, where the bimolecular reaction of $\text{HCo}(\text{CO})_4$ and $\text{RCOCo}(\text{CO})_4$ leads to $\text{Co}_2(\text{CO})_8$ and aldehyde (eq 1).



Subsequent studies with unmodified cobalt failed to support significant product formation from such a mechanism.¹⁷ In addition, initial in situ spectroscopic studies with unmodified rhodium and cyclohexene failed to support any statistically significant product formation from such a mechanism.¹⁸ Interest in homometallic and hetero-bimetallic stoichiometric binuclear elimination and in the possible existence of the catalytic binuclear elimination reaction (CBER) has been the focus of

numerous studies for more than 2 decades.^{19–22} Importantly, it has been pointed out that mononuclear hydride complexes might have particular affinity for free coordination sites on other metal complexes, leading to bimolecular reaction and simultaneous product formation.^{20b}

The existence of a Heck–Breslow (II) mechanism, e.g., a catalytic binuclear elimination reaction, has considerable importance. First, it changes the frequent assumption that “homogeneous catalysis” automatically implies a unicyclic reaction mechanism. Second, the bimetallic case provides a sophisticated mechanistic basis for synergism, one that does not rely on cluster catalysis.²³ Third, the bimetallic case changes the frequent working assumption that in order to modify an existing homogeneous catalytic system, a new ligand should be designed and tested. Fourth, both homometallic and hetero-bimetallic systems have the potential for highly nonlinear kinetics, in particular, linear-quadratic and linear-bilinear kinetics.^{24,25} In the rate-limiting cases, the reactions of two homometallic complexes or two hetero-bimetallic complexes in the product formation step introduce quadratic and bilinear terms, respectively. Thus both forms provide unique opportunities for better metal utilization, especially when the frequently used but rather scarce precious metals Pd, Ru, Rh, Os, Ir, and Pt are involved.

Recently, detailed in situ spectroscopic studies of both homometallic and hetero-bimetallic rhodium catalyzed hydroformylations showing anomalous behavior have been performed.²⁵ Statistically significant product formation was shown to correlate with the bimolecular events $[\text{HRh}(\text{CO})_4][\text{RCORh}(\text{CO})_4]$ and $[\text{HMn}(\text{CO})_5][\text{RCORh}(\text{CO})_4]$, but crucial dinuclear intermediates were not observed during reaction. The simultaneous observation of both mononuclear and dinuclear intermediates, as well as detailed kinetics supporting their simultaneous

- (12) Marko, L. *Aspects Homogeneous Catal.* **1974**, *2*, 3–55.
 (13) Dickson, R. S. *Homogeneous Catalysis with compounds of Rhodium and Iridium*; D. Reidel Publishing Company: Dordrecht, Holland, 1985.
 (14) Li, C.; Widjaja, E.; Chew, W.; Garland, M. *Angew. Chem., Int. Ed.* **2002**, *20*, 3785–3789.
 (15) Garland, M.; Bor, G. *Inorg. Chem.* **1989**, *28* (3), 410–13.
 (16) (a) Garland, M.; Pino, P. *Organometallics* **1990**, *10*, 1693–1704. (b) Liu, G.; Volken, R.; Garland, M. *Organometallics* **1999**, *18*, 3429–3436. (c) Feng, J.; Garland, M. *Organometallics* **1999**, *18* (3), 417–427.
 (17) Mirbach, M. F. *J. Organomet. Chem.* **1984**, *265* (2), 205–13.
 (18) Feng, J.; Garland, M. *Organometallics* **1999**, *18*, 1542–1546.

- (19) (a) von Brandes, K. H.; Jonassen, H. B. *Z. Anorg. Allg. Chem.* **1966**, *343*, 215–219. (b) Ungvary, F.; Marko, L. *J. Organomet. Chem.* **1969**, *20*, 205–209. (c) Byers, B. H.; Brown, T. L. *J. Am. Chem. Soc.* **1977**, *99*, 2528–2532. (d) Ungvary, F.; Marko, L. *Organometallics* **1983**, *2*, 1608–1612. (e) Hoff, C.; Ungvary, F.; King, R. B.; Marko, L. *J. Am. Chem. Soc.* **1985**, *107*, 666–671. (f) Norton, J. R.; Carter, W.; Kelland, J.; Okrasinski, S. *Adv. Chem. Ser.* **1978**, *167*, 170–180. (g) Edidin, R. T.; Hennessy, K.; Moody, A.; Okrasinski, S.; Norton, J. R. *New J. Chem.* **1988**, *12*, 475–477. (h) Nappa, M. J.; Santi, R.; Diefenbach, S.; Halpern, J. *J. Am. Chem. Soc.* **1982**, *104*, 619–621. (i) Nappa, M. J.; Santi, R.; Halpern, J. *Organometallics* **1985**, *4*, 34–41. (j) Brown, C. K.; Georgiou, D.; Wilkinson, G. *J. Chem. Soc. A* **1971**, 3120–3127. (k) Schwartz, J.; Cannon, J. *J. Am. Chem. Soc.* **1974**, *96*, 4721. (l) Barborak, J. C.; Cann, K. *Organometallics* **1982**, *1*, 1726–1728.
 (20) (a) Kovacs, I.; Ungvary, F.; Marko, L. *Organometallics* **1986**, *5* (2), 209–15. (b) Norton, J. R. *Acc. Chem. Res.* **1979**, *12*, 139–145. (c) Mitchell, Christina M.; Stone, F. G. A. *J. Chem. Soc. Dalton Transactions: Inorg. Chem.* **1972**, *11* (J), 102–7. (d) Renaut, P.; Tainturier, G.; Gautheron, B. *J. Organomet. Chem.* **1978**, *150* (1), C9–C10. (e) Martin, Bruce; Warner, D. K.; Norton, J. R. *J. Am. Chem. Soc.* **1986**, *108* (1), 33–39. (f) Hoxmeier, R. J.; Blickensderfer, J. R.; Kaez, H. D. *Inorg. Chem.* **1979**, *18*, 3453–3461. (g) Kovacs, I.; Hoff, C. D.; Ungvary, F.; Marko, L. *Organometallics* **1985**, *4*, 1347–1350.
 (21) (a) Jones, W. D.; Bergman, R. G. *J. Am. Chem. Soc.* **1979**, *101* (18), 5447–9. (b) Jones, W. D.; Huggins, J.; Bergman, R. G. *J. Am. Chem. Soc.* **1981**, *103*, 4415–4423. (c) Collman, J. P.; Belmont, J.; Brauman, J. *J. Am. Chem. Soc.* **1983**, *105*, 7288–794. (d) Beletskaya, I. P.; Voskoboinikov, A. Z.; Magomedov, G. K. *Metalloorg. Khim.* **1989**, *2* (4), 810–13. (e) Beletskaya, I. P.; Magomedov, G. K.; Voskoboinikov, A. Z. *J. Organomet. Chem.* **1990**, *385*, 289–295.
 (22) Collman, J. P.; Hegedus, L. S.; Norton, J. R.; Finke, R. G. *Principles and Applications of Organotransition Metal Chemistry*; University Science Books: Mill Valley, CA, 1987.
 (23) Adams, R. D.; Albert Cotton, F., Eds. *Catalysis by di- and polynuclear metal cluster complexes*; Wiley: New York, 1998.
 (24) Leong, M. L. Kinetic polynomials of the homogeneous bimetallic catalytic elimination reaction, B. Eng. Thesis, National University of Singapore, 1999.
 (25) (a) Li, C.; Widjaja, E.; Garland, M. *J. Am. Chem. Soc.* **2003**, *125*, 5540–5548. (b) Li, C.; Widjaja, E.; Garland, M. *Organometallics* **2004**, *23*, 4131–4138. (c) Liu, G.; Li, C.; Guo, L.; Garland, M. *J. Catal.* **2006**, *237*, 67–78.

involvement in the same reaction mechanism, would lend rather conclusive support to the concept of a catalytic binuclear elimination reaction. In turn, this would help to change some frequent working assumptions in homogeneous catalysis and promote the search for and development of CBER type mechanisms for other organic syntheses.

In the present rhodium and rhenium hetero-bimetallic system, both mononuclear and dinuclear intermediates are observed by in situ infrared spectroscopy during hydroformylation of cyclopentene. The hydroformylation kinetics correlate with not only the bimolecular event $[\text{HRe}(\text{CO})_5][\text{RCORh}(\text{CO})_4]$ but also the hydrogen activation by the observed species $\text{RhRe}(\text{CO})_9$. The observable product formation arises from the existence of both a unicyclic rhodium catalytic cycle and a hetero-bimetallic rhodium–rhenium CBER. The observable rate constant for the rate-limiting step of the CBER was significantly greater than the observable rate constant for the unicyclic reaction mechanism. Thus the addition of less expensive rhenium, and the presence of a CBER mechanism, has dramatically increased the utilization of the scarce precious metal rhodium.

Results

Signal Processing and BTEM Analysis. Individual catalytic runs (22) were carried out in batch mode with in situ FTIR measurements according to the procedure described in the Experimental and Numerical Aspects section. The resulting 763 in situ FTIR absorbance spectra were first subjected to singular value decomposition (SVD)²⁶ in order to determine the associated basis vectors (see Supporting Information for details). Then band-target entropy minimization (BTEM)²⁷ was applied to the SVD results in order to recover pure component spectral estimates of the constituents present. BTEM was able to recover good spectral estimates of the solvent *n*-hexane and the dissolved CO, as well as the moisture in the sample chamber. In addition, as shown in Figure 1, BTEM recovered the pure component organic and organometallic solutes present during the hydroformylations. The recovered pure component spectra include the reagents used, namely $\text{Rh}_4(\text{CO})_{12}$, cyclopentene, and $\text{HRe}(\text{CO})_5$. In addition, two further organometallic species were identified, $\text{RCORh}(\text{CO})_4$ and $\text{RhRe}(\text{CO})_9$, and one organic species cyclopentane carboxaldehyde. The organorhodium species $\text{RCORh}(\text{CO})_4$ was first identified in 1989 under hydroformylation conditions,¹⁵ and $\text{RhRe}(\text{CO})_9$ was recently synthesized and characterized under CO.²⁸ All spectral estimates possess excellent signal-to-noise ratios. The spectral estimates of the isolatable species such as cyclopentene, $\text{Rh}_4(\text{CO})_{12}$, $\text{HRe}(\text{CO})_5$, and cyclopentane carboxaldehyde are in excellent agreement with authentic references. Further analysis of the spectroscopic data did not provide any support for the presence of observable quantities of $\text{Rh}_6(\text{CO})_{16}$,²⁹ $\text{HRh}(\text{CO})_4$,¹⁴ or $\text{Re}_2(\text{CO})_{10}$.³⁰

In Situ Concentration Profiles. After obtaining the pure component spectral estimates via BTEM, the time-dependent

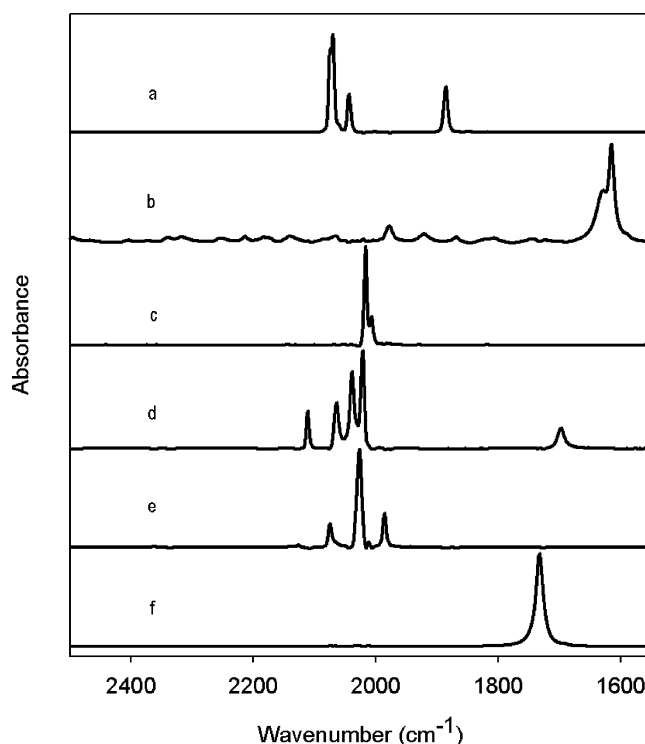


Figure 1. BTEM spectral estimates of the organic and organometallic solutes present during the active catalytic hydroformylation experiments: (a) $\text{Rh}_4(\text{CO})_{12}$, (b) cyclopentene, (c) $\text{HRe}(\text{CO})_5$, (d) $\text{RCORh}(\text{CO})_4$, (e) $\text{RhRe}(\text{CO})_9$, (f) cyclopentane carboxaldehyde.

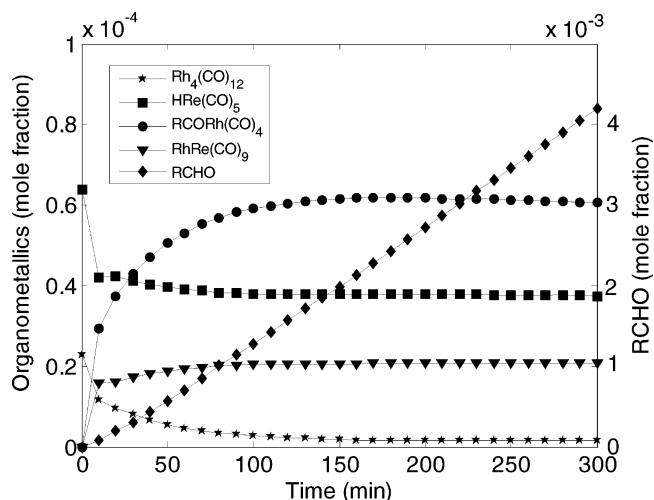


Figure 2. Time-dependent mole fractions of the organometallic solutes and organic product cyclopentane carboxaldehyde. In this standard experiment, the initial reaction conditions were 42.49 mg of $\text{Rh}_4(\text{CO})_{12}$, 20 μL of $\text{HRe}(\text{CO})_5$, 5.5 mL of cyclopentene in 300 mL of hexane with 4.0 MPa CO and 1.0 MPa H_2 . The experiment was isothermal at 289.7 K, and due to the large gas-phase volume, the total pressure change in the system was less than 2% during this 300 min experiment. Only ca. 15% conversion of the alkene occurs during this experiment.

moles of solute species and their time-dependent mole fractions were obtained by algebraic optimization techniques (see Experimental and Numerical Aspects section for details). The concentration profiles of the organometallic solutes and the organic product for a typical bimetallic hydroformylation experiment at 289.7 K are shown in Figure 2. Due to the multivariate methods used, the concentration profiles show little if any scatter, in spite of the very low organometallic loadings used, and the small signal intensities involved. The concentra-

(26) Golub, G. H.; Van Loan, C. F. *Matrix Computations*, 3rd ed.; Johns Hopkins University Press: Baltimore, MD, 1996.

(27) (a) Chew, W.; Widjaja, E.; Garland, M. *Organometallics* **2002**, *21*, 1882–1890. (b) Widjaja, E.; Li, C.; Garland, M. *Organometallics* **2002**, *21*, 1991–1997.

(28) Li, C.; Guo, L.; Garland, M. *Organometallics* **2004**, *23*, 5275–5279.

(29) Chini, P. *Chem. Commun.* **1967**, 440–1.

(30) Cotton, F. A.; Liehr, A. O.; Wilkinson, G. J. *Inorg. Nucl. Chem.* **1956**, *2*, 141–148.

tions of the organometallic precursors $\text{Rh}_4(\text{CO})_{12}$ and $\text{HRe}(\text{CO})_5$ decline rapidly, and the concentrations of the other observable organometallics $\text{RCORh}(\text{CO})_4$ and $\text{RhRe}(\text{CO})_9$ increase rapidly after the reactions start. A significant portion of the transient behavior is finished in ca. 50 min, and the organometallic solutes have achieved their asymptotic limits/concentrations within ca. 100 min. At ca. 100 min, almost all $\text{Rh}_4(\text{CO})_{12}$ precursor has disappeared, and only mononuclear and dinuclear species remain.

Measurable quantities of the hydroformylation product, cyclopentane carboxaldehyde, were already observed in the first 10 min. Thereafter, the rate of product formation is essentially constant. Only a small induction period is seen at the start of the experiment. At 10 min, 1.99×10^{-4} mol of cyclopentane carboxaldehyde has been produced. Since the total loading of the precursors resulted in 2.51×10^{-4} mol of metal, nearly one turnover of the system has already occurred at 10 min at this low hydroformylation temperature of 289.7 K.

The absence of observable $\text{Re}_2(\text{CO})_{10}$ is a strong indication that radical mechanisms involving rhenium are not significant or even absent in this *n*-hexane solution, since $\text{Re}_2(\text{CO})_{10}$ is known to readily form from mononuclear rhenium carbonyl radicals.^{20c} In addition, independent hydroformylation experiments conducted with both $\text{Rh}_4(\text{CO})_{12}$ and $\text{Re}_2(\text{CO})_{10}$ as catalytic precursors showed no measurable formation of $\text{HRe}(\text{CO})_5$ or $\text{RhRe}(\text{CO})_9$.

Precatalytic Steps. It is known that the precatalytic kinetics of unmodified rhodium-catalyzed hydroformylation are governed by the need to form the species $\{\text{Rh}_4(\text{CO})_{14}\}$ followed by hydrogen activation.¹⁶ In addition, it is known that the induction period for simple alkene hydroformylation using $\text{Rh}_4(\text{CO})_{12}$ is ca. 4 h at conditions similar to those used in this study.³¹ In the present bimetallic hydroformylations, the conversion of $\text{Rh}_4(\text{CO})_{12}$ to $\text{RCORh}(\text{CO})_4$ occurred much more rapidly, i.e., ca. 1.5 h.

The formation of $\text{RCORh}(\text{CO})_4$ was modeled using eq 2 where all concentrations are expressed in mole fractions. Regression of the initial data provided rate constants $k_1 = (3.0 \pm 0.5) \times 10^2 \text{ min}^{-1}$ and $k_2 = (6.2 \pm 1.5) \times 10^4 \text{ min}^{-1}$, where the errors are listed as twice the standard deviation, i.e., the 95% confidence limit. This result indicates that the attack of $\text{HRe}(\text{CO})_5$ on $\{\text{Rh}_4(\text{CO})_{14}\}$ is ca. 200 times more effective than the reaction of molecular hydrogen with $\{\text{Rh}_4(\text{CO})_{14}\}$. The first term k_1 is consistent with a previous manganese–rhodium hydroformylation of cyclopentene at 289.7 K where the value $k_1 = (4.0 \pm 0.8) \times 10^2 \text{ min}^{-1}$ was obtained.^{25b}

$$\begin{aligned} \frac{d[\text{RCORh}(\text{CO})_4]}{dt} = & k_1[\text{Rh}_4(\text{CO})_{12}][\text{CO}]^2[\text{H}_2] + \\ & k_2[\text{Rh}_4(\text{CO})_{12}][\text{CO}]^2[\text{HRe}(\text{CO})_5] \quad (2) \end{aligned}$$

The equilibration of tetranuclear carbonyl complexes with open polyhedra has been invoked on previous occasions in order to rationalize the kinetics of metal carbonyl cluster transformations.³² In the present case, the subsequent attack of metal hydride is much more rapid and effective than the attack of molecular hydrogen. Since these two steps are the rate-limiting steps for the formation of the acyl species, subsequent details

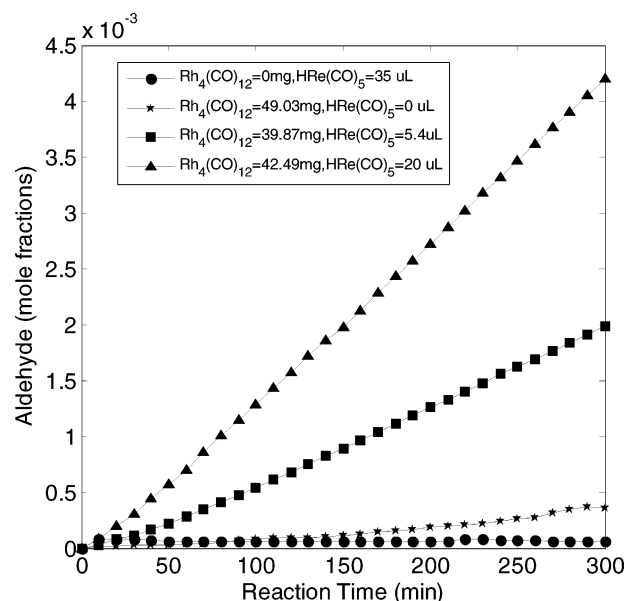


Figure 3. Effect of changing rhenium concentrations on rate of hydroformylation: a comparison of the time-dependent mole fractions of the organic product cyclopentane carboxaldehyde from 4 of the 22 hydroformylation experiments. The other initial reaction conditions were the same, namely, 5.5 mL of cyclopentene in 300 mL of hexane with 4.0 MPa CO and 1.0 MPa H_2 at 289.7 K

of the remaining elementary steps are lost. The reasons for the efficiency of metal hydride attack on $\{\text{Rh}_4(\text{CO})_{14}\}$ may include the particular affinity mononuclear hydride complexes have for free coordination sites on other complexes.^{20b}

Hydroformylation Rates. Figure 3 shows the time-dependent concentrations of cyclopentane carboxaldehyde formed in four representative hydroformylation experiments all conducted at 289.7 K, 4.0 MPa CO, and 1.0 MPa H_2 . The monometallic hydroformylations, involving only rhenium or rhodium, are used as the base cases. The results of the standard experiment (Exp 5) are also included, as well as one additional experimental Exp 6 (see Table 1 in the Experimental and Numerical Aspects section for details). Again, the concentration profiles show very little scatter. The rates of hydroformylations were $(2.8 \pm 6.4) \times 10^{-8}$, 1.28×10^{-6} , 6.87×10^{-6} , and 1.41×10^{-5} mol fraction/min, with pure rhenium, pure rhodium, Exp 6 ($\text{HRe}(\text{CO})_5 = 5.4 \mu\text{L}$), and Exp 5 ($\text{HRe}(\text{CO})_5 = 20.0 \mu\text{L}$), respectively. The turnover frequencies (TOFs) based on rhodium acyl were 0.03 ± 0.01 , 0.11 ± 0.01 , and $0.25 \pm 0.02 \text{ min}^{-1}$ when the initial loadings of $\text{HRe}(\text{CO})_5$ were 0, 5.4, and 20.0 μL , respectively. These results clearly show that pure rhenium has essentially no catalytic activity, but that bimetallic rhodium and rhenium experiments are much more active than the pure rhodium hydroformylations.

The dramatic and synergistic effect of rhenium on the hydroformylations can be further demonstrated. In Figure 3, when the rhenium to rhodium ratios were 0.75:1 ($\text{HRe}(\text{CO})_5 = 5.4 \mu\text{L}$) and 2.58:1 ($\text{HRe}(\text{CO})_5 = 20.0 \mu\text{L}$), respectively, the rates of hydroformylation were ca. 5.5 and 12 times greater than that for the pure rhodium experiment. Thus the addition of approximately equimolar amounts of rhenium carbonyl hydride (inactive in its pure form) promoted the already excellent activity of rhodium by ca. 1 order of magnitude.

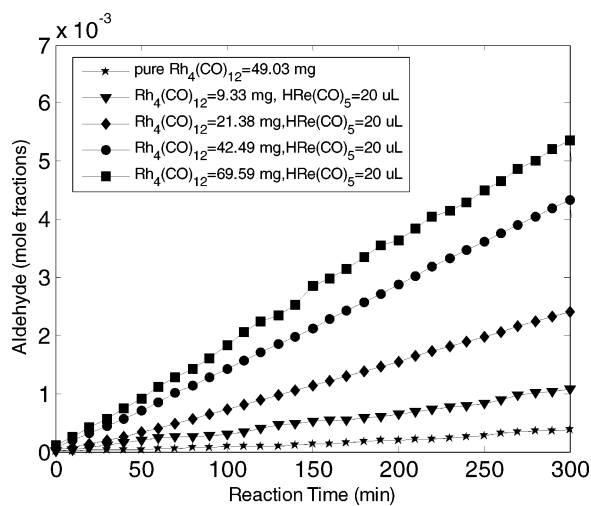
A similar series of experiments were conducted at fixed rhenium concentrations but variable rhodium concentrations.

(31) Garland, M. *Organometallics* **1993**, *12*, 535–543.

(32) (a) Bor, G.; Dietler, U. K.; Pino, P.; Poe, A. J. *Organomet. Chem.* **1978**, *154*, 301–315. (b) Ungvary, F.; Marko, L. *Inorg. Chim. Acta* **1970**, *4*, 324–326.

Table 1. Experimental Design for the in Situ Spectroscopic and Kinetic Study of the Bimetallic Hydroformylation of Cyclopentene Starting with Rh₄(CO)₁₂ and HRe(CO)₅ Precursors

exp no.	HRe(CO) ₅ , μL	Rh ₄ (CO) ₁₂ , mg	CP, mL	CO, MPa	H ₂ , MPa	temp, K	remarks
1	0	0	5.5	4.0	1.0	289.7	blank
2	20.0	0	5.5	2.0	2.0	294.3	pure HRe(CO) ₅ 1
3	35.0	0	5.5	4.0	1.0	289.7	pure HRe(CO) ₅ 2
4	0	49.03	5.5	4.0	1.0	289.7	pure Rh ₄ (CO) ₁₂
5	20.0	42.49	5.5	4.0	1.0	289.7	standard exp
6	5.4	39.87	5.5	4.0	1.0	289.7	HRe(CO) ₅ variation
7	15.0	39.37	5.5	4.0	1.0	289.7	
8	40.0	39.90	5.5	4.0	1.0	289.7	
9	20.0	9.33	5.5	4.0	1.0	289.7	Rh ₄ (CO) ₁₂ variation
10	20.0	21.38	5.5	4.0	1.0	289.7	
11	20.0	69.59	5.5	4.0	1.0	289.7	
12	20.0	37.89	3.0	4.0	1.0	289.7	cyclopentene variation
13	20.0	40.40	15.0	4.0	1.0	289.7	
14	20.0	37.17	5.5	3.0	1.0	289.7	CO variation
15	20.0	37.42	5.5	5.0	1.0	289.7	
16	20.0	39.42	5.5	6.0	1.0	289.7	
17	20.0	38.14	5.5	4.0	0.5	289.7	H ₂ variation
18	20.0	38.67	5.5	4.0	1.5	289.7	
19	20.0	38.07	5.5	4.0	2.0	289.7	
20	20.0	40.02	5.5	4.0	1.0	282.6	temperature variation
21	19.0	40.43	5.5	4.0	1.0	294.0	
22	18.5	37.70	5.5	4.0	1.0	298.5	

**Figure 4.** Effect of changing rhodium concentrations on rate of hydroformylation: a comparison of the time-dependent mole fractions of the organic product cyclopentane carboxaldehyde from 5 of the 22 hydroformylation experiments. The other initial reaction conditions were the same, namely, 5.5 mL of cyclopentene in 300 mL of hexane with 4.0 MPa CO and 1.0 MPa H₂ at 289.7 K

This series showed regular increases in hydroformylation rates with increasing rhodium concentrations (Figure 4). Particular noteworthy is the fact that the rate of hydroformylation with 9.33 mg of Rh₄(CO)₁₂ in the presence of HRe(CO)₅ is more than twice the rate of hydroformylation with 49.03 mg of Rh₄(CO)₁₂ alone.

Hydroformylation Kinetics. Since the hydroformylation rates show a dependence in both rhodium and rhenium, it is assumed that two simultaneous mechanisms occur for product formation. These are the hydrogenolysis of the acyl rhodium tetracarbonyl RCORh(CO)₄ and the bimolecular reaction of RCORh(CO)₄ and HRe(CO)₅. Equation 3 is the ordinary

differential equation describing total aldehyde formation. The reaction orders for hydrogenolysis are known from the literature.¹⁶ This leaves three unknowns, namely the two rate constants and the reaction order in CO for the binuclear elimination.

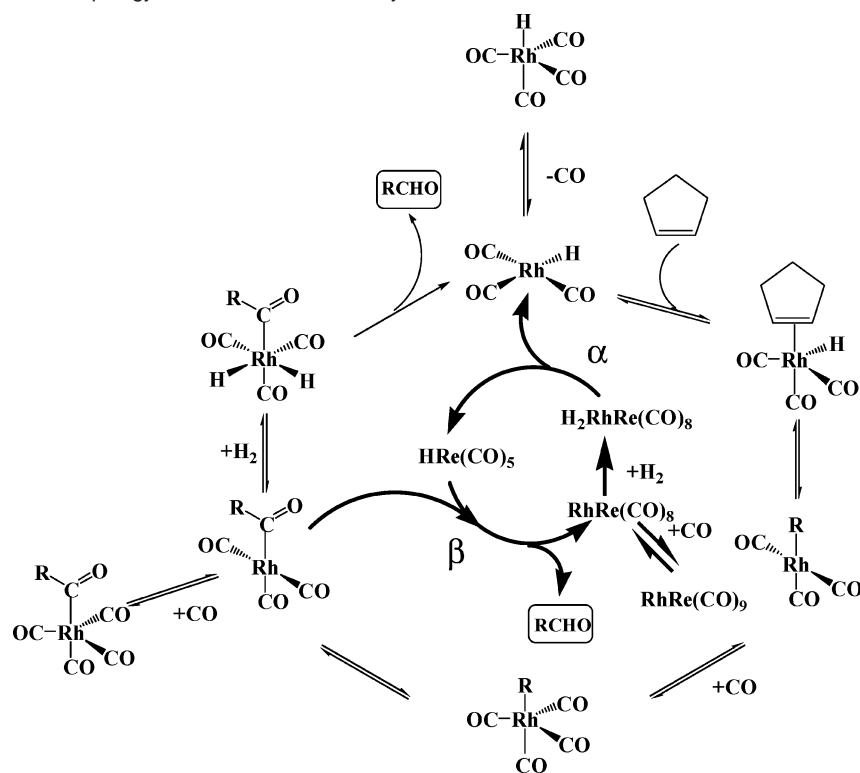
$$r_{\text{Total}} = k_3[\text{RCORh}(\text{CO})_4][\text{H}_2][\text{CO}]^{-1} + k_4[\text{RCORh}(\text{CO})_4][\text{HRe}(\text{CO})_5][\text{CO}]^x \quad (3)$$

The experimental design for this study (1) covered a range of rhodium, rhenium, alkene, CO, and hydrogen concentrations; (2) the rates of total aldehyde formation were measured at a variety of conditions; and (3) the corresponding organometallic concentrations were measured in situ. Accordingly, eq 3 can be properly regressed. Mole fractions were used for the concentrations of all solutes. A nonlinear regression of data measured at 289.7 K provided $k_3 = 0.33 \pm 0.04 \text{ min}^{-1}$, $k_4 = 110 \pm 12 \text{ min}^{-1}$, and $x = -1.60 \pm 0.04$. The value of k_3 is consistent with the pure rhodium experiment carried out in this study $0.30 \pm 0.03 \text{ min}^{-1}$ as well as the previously reported value of $0.314 \pm 0.08 \text{ min}^{-1}$.^{25b} The reaction order for the binuclear elimination suggests coordinative unsaturation on one and possibly both organometallics, and the rate constant has reasonable confidence limits. These parameters indicate that ca. 80% of the product formation in the standard experiment (Exp 5) arises from a catalytic binuclear elimination reaction.

The terms in eq 3 can be rearranged as $k_3[\text{CO}]^{-1}/k_4[\text{CO}]^{-1.6}$ to compare the attack of either molecular hydrogen or HRe(CO)₅ on RCORh(CO)₄. At the mean carbon monoxide partial pressures used in this study, HRe(CO)₅ is ca. 1200 times more effective than molecular hydrogen as a reactant for aldehyde formation! This represents a dramatically improved utilization of rhodium. As further clarification, it can be noted that the mean mole fractions of molecular hydrogen and HRe(CO)₅ in this study are on the order of 10⁻² and 10⁻⁵ mole fractions, respectively, yet the binuclear elimination is the main contributor to product formation.

Interconnected Unicyclic and CBER Mechanisms. The hydroformylation kinetics indicates that two pathways are available for aldehyde formation. These are a classic mononuclear mechanism and a rhodium–rhenium bimetallic catalytic binuclear elimination reaction. Since some of the intermediates in both mechanisms are the same, the two mechanisms are coupled. The combined mechanisms are shown in Scheme 2. The elementary steps α and β are crucial for the existence of the CBER mechanism. The step α provides activation of molecular hydrogen and cleaves the hetero-bimetallic intermediate back to mononuclear intermediates, and the β step is the binuclear elimination between mononuclear intermediates to give a dinuclear intermediate and organic product formation.

Hydrogen Activation by RhRe(CO)₉. The basic features of the proposed reaction topology in Scheme 2 can be further investigated and confirmed by analyzing the kinetics of hydrogen activation by RhRe(CO)₉. As shown by eq 3, the overall hydroformylation rates can be partitioned into the contribution from the rhodium cycle and the Rh–Re CBER. In turn, correspondence should exist between the rate of Rh–Re CBER hydroformylation and hydrogen activation by RhRe(CO)₉. The ordinary differential equation relating the variables involved is given in eq 4, where the first term on the right-hand side

Scheme 2. Proposed Reaction Topology for Inter-connected Unicyclic and CBER Mechanisms^a

^a The elementary reactions α and β involve the interconversion of mononuclear and dinuclear organometallics. The species $\text{RCORh}(\text{CO})_4$, $\text{HRe}(\text{CO})_5$, and $\text{RhRe}(\text{CO})_9$ are observable organometallics in the present system, and $\text{HRh}(\text{CO})_4$ has been previously observed during hydroformylations.^{25c}

represents the rate of hydroformylation from the Rh–Re CBER and the second term is the rate of hydrogen activation by $\text{RhRe}(\text{CO})_9$. At pseudo-steady state, the concentration of $\text{RhRe}(\text{CO})_9$ is constant as indicated by the data in Figure 2 and hence the rate of change of $\text{RhRe}(\text{CO})_9$ is zero. The corresponding algebraic equation can then be solved for one unknown, namely k_5 .

$$\frac{d[\text{RhRe}(\text{CO})_9]}{dt} = k_4[\text{RCORh}(\text{CO})_4][\text{HRe}(\text{CO})_5][\text{CO}]^x - k_5[\text{RhRe}(\text{CO})_9][\text{H}_2][\text{CO}]^{-1} \approx 0 \quad (4)$$

The same type of analysis can be performed for the pseudo steady state concentrations of $\text{HRe}(\text{CO})_5$ and even $\text{RCORh}(\text{CO})_4$. The resulting mathematical expressions have only one unknown, namely k_5 . Therefore, it is sufficient to model only one pseudo-steady-state concentration in order to describe the pseudo steady state behavior.

Pseudo-steady-state data for the organometallics can be obtained for all the bimetallic hydroformylations in the interval of ca. 100–300 min. Figure 5 shows the time-dependent concentrations of the rhenium organometallics $\text{HRe}(\text{CO})_5$ and $\text{RhRe}(\text{CO})_9$ for four representative experiments. Indeed, very little variation in the concentrations is observed in the period 100–300 min.

Regression of the data provided a value for the observable rate constant k_5 of $3.81 \pm 0.07 \text{ min}^{-1}$. The high confidence limits for the rate constant strongly suggest that the present hydroformylation results arise from a combined classic mononuclear rhodium mechanism and a CBER mechanism as shown in Scheme 2. Indeed, the hydrogen activation kinetics confirms that the dinuclear species $\text{RhRe}(\text{CO})_8$ and $\text{RhRe}(\text{CO})_9$ are essential for product formation. The rate of hydrogen activation

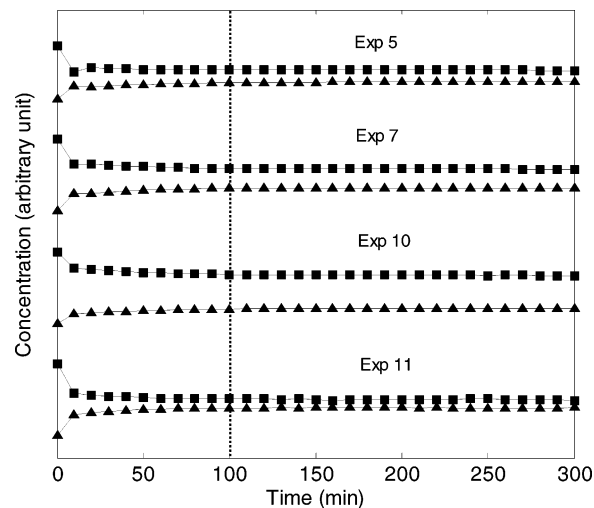


Figure 5. Concentrations of the rhenium organometallics $\text{HRe}(\text{CO})_5$ (■) and $\text{RhRe}(\text{CO})_9$ (▲) for four representative bimetallic catalytic hydroformylations: Exp 5, Exp 7, Exp 10, and Exp 11. After the rapid initial transient behavior, a pseudo-steady state for the organometallics can be identified in the interval of ca. 100–300 min.

on $\text{RhRe}(\text{CO})_8/\text{RhRe}(\text{CO})_9$ is exactly equal to the rate of CBER hydroformylation. The transformations of the observed monometallic and dinuclear organometallics are synchronized, and together they are responsible for hydroformylation.

A comparison can be made between the rate of hydrogen activation on $\text{RCORh}(\text{CO})_4$ and the rate of hydrogenation activation on $\text{RhRe}(\text{CO})_9$, using the products $k_3[\text{RCORh}(\text{CO})_4][\text{H}_2][\text{CO}]^{-1}$ and $k_5[\text{RhRe}(\text{CO})_9][\text{H}_2][\text{CO}]^{-1}$ in eqs 3 and 4. It is found that the rate of hydrogen activation due to the second term is ca. 4 times greater than the first term, which is consistent

with the fact that ca. 80% of product formation came from CBER at the mean reaction conditions used in this study.

The complex $\text{RhRe}(\text{CO})_9$ exhibits an unusually high rate of hydrogen activation. Indeed, the observable rate constant $k_{\text{obsd}} \approx 38 \text{ min}^{-1}$ under the mean CO partial pressure of 4.0 MPa compares very favorably with many complexes used as catalyst precursors in catalytic hydrogenation. For example, the observable rate constant of the benchmark Vaska complex $\text{IrCl}(\text{CO})(\text{PPh}_3)_2$ is ca. 420 min^{-1} under zero CO partial pressure.³³ The difficulty of activating molecular hydrogen in the presence of CO has been noted before.³⁴ The ability of some hetero-bimetallic complexes to readily activate molecular hydrogen at ambient temperature has also been noted before and attributed to the polarization of the hydrogen bond during cleavage, thus lowering the activation energy.^{35,36} The observable rate constant k_{obsd} for $\text{RhRe}(\text{CO})_9$ is comparable to $k_{\text{obsd}} = 66 \text{ min}^{-1}$ observed with $\text{RhCo}(\text{CO})_7$ which also activates molecular hydrogen readily in the presence of CO.³⁷ The facile hydrogen activation kinetics of $\text{RhRe}(\text{CO})_9$ play a significant role in the present rapid CBER kinetics.

Isotopic Labeling. Triply labeled cyclopentane carboxaldehyde $\text{CH}_2\text{CH}_2\text{CH}_2\text{CHDCH} - {}^{13}\text{CDO}$ instead of cyclopentene was used in an experiment conducted at otherwise standard conditions, hence, in the presence of $\text{Rh}_4(\text{CO})_{12}$, $\text{HRe}(\text{CO})_5$, carbon monoxide, and hydrogen at 289.7 K. As expected, the dinuclear species $\text{RhRe}(\text{CO})_9$ was rapidly formed under these conditions. No experimental evidence was obtained for decarboxylation or hydroformylation reversibility in the 5 h experiments. Specifically, there was no spectroscopic evidence for (1) the removal/exchange of the deuterium on the carbonyl, i.e., transformation of $\text{CH}_2\text{CH}_2\text{CH}_2\text{CHDCH} - {}^{13}\text{CDO}$ to $\text{CH}_2\text{CH}_2\text{CH}_2\text{CHDCH} - {}^{13}\text{CHO}$ and hence a shift of the carbonyl vibration from 1722 cm^{-1} , (2) the decarbonylation of $\text{CH}_2\text{CH}_2\text{CH}_2\text{CHDCH} - {}^{13}\text{CDO}$ followed by recarbonylation to form $\text{CH}_2\text{CH}_2\text{CH}_2\text{CHDCH} - {}^{12}\text{CDO}$ or $\text{CH}_2\text{CH}_2\text{CH}_2\text{CHDCH} - {}^{12}\text{CHO}$ and hence a shift of the carbonyl vibration from 1722 cm^{-1} to 1733 cm^{-1} , and (3) the formation of alkene; i.e., no new signals at ca. 1640 cm^{-1} appeared. Furthermore, no significant changes in the metal carbonyl vibrations of $\text{Rh}_4(\text{CO})_{12}$, $\text{HRe}(\text{CO})_5$, and $\text{RhRe}(\text{CO})_9$ were observed. Taken together, the results suggest that neither significant decarbonylation nor hydroformylation reversibility exists in this system at 289.7 K. This result is consistent with other hydroformylation studies using (1) cobalt where little reversibility of the hydroformylation reaction was observed at elevated temperatures, i.e., 423–473 K,¹⁰ and (2) Pt–Sn systems where essentially irreversible hydroformylation occurs at 39 °C and reversibility is observed at 98 °C.¹¹

Discussion

In large part, the detailed results of the present study were only made possible due to the special signal processing

techniques used. In particular, band-target entropy minimization allowed outstanding spectral recovery of the observable organic and organometallic species present. Many of the organometallics observed were in fact nonisolatable intermediates in the catalysis, particularly $\text{RCORh}(\text{CO})_4$ and $\text{RhRe}(\text{CO})_9$. In addition, the algebraic system identification techniques permitted excellent quantitative information. Indeed, the resulting time-dependent concentration profiles are very smooth, even for the organometallic species, whose mean concentrations were on the order of 30 ppm. In turn, this high quality in situ spectroscopic analysis then permitted detailed kinetic modeling of the induction period, the catalysis, and hydrogen activation. These phenomena could be numerically decoupled and separately analyzed.

In the present study, the addition of $\text{HRe}(\text{CO})_5$ to the unmodified rhodium-catalyzed hydroformylation resulted in a dramatic increase in the rate of aldehyde formation. The in situ spectroscopic measurements showed that the presence of $\text{HRe}(\text{CO})_5$, $\text{RCORh}(\text{CO})_4$, and $\text{RhRe}(\text{CO})_9$ were correlated with the system activity. Detailed modeling showed that there were two contributions to aldehyde formation, namely hydrogenolysis of $\text{RCORh}(\text{CO})_4$ and the bimolecular reaction of $\text{HRe}(\text{CO})_5$ and $\text{RCORh}(\text{CO})_4$. Thus, at this level of analysis, the catalytic system appears to consist of a classic unmodified mononuclear rhodium mechanism together with a Heck–Breslow II mechanism.

Moreover, the rate of hydrogen activation of $\text{RhRe}(\text{CO})_9$ was *synchronized* with the rate of aldehyde formation arising from bimolecular reaction of $\text{HRe}(\text{CO})_5$ and $\text{RCORh}(\text{CO})_4$. This result provides conclusive evidence for the simultaneous existence of both mononuclear and dinuclear organometallics in a single homogeneous catalytic mechanism. In other words, this synchronization of events confirms the existence of a Heck–Breslow II or catalytic binuclear elimination mechanism. The concentrations of $\text{HRe}(\text{CO})_5$, $\text{RCORh}(\text{CO})_4$, and $\text{RhRe}(\text{CO})_9$ are all coupled and interdependent, and these three species act in a concerted and collective manner to give rise to product formation.

The ratio of the observable rate constants from the CBER and unicyclic mechanisms is ca. 1200 at the mean conditions of this study. Thus the catalytic binuclear elimination reaction mechanism is extraordinarily more efficient than the classic unicyclic mechanism with respect to the utilization of rhodium, the metal of choice for catalytic hydroformylation. Catalytic binuclear elimination is the phenomenological basis for the observed synergism of the bimetallic system.

There are broader implications that should be explored in the future. Hetero-bimetallic catalytic binuclear elimination represents a new and possibly rather general synthetic option. Indeed, it differs with the widely used approach of organic ligand design/modification in order to achieve new metal-mediated synthetic avenues. Hetero-bimetallic CBER might be developed for already known systems, by the addition of an appropriate second metal complex. Furthermore, the bilinear term provides the potential for achieving greater utilization of the (precious) metals used. Thus, it might be possible to significantly reduce the amount of precious metal used or, if preferred, achieve a significantly higher volumetric rate of product formation for the same loading of precious metal (bilinear advantage). From a topological viewpoint, hetero-bimetallic CBERs should be stable and not exhibit instabilities or bifurcation.³⁸ Hence the nonlinearity of such systems does not appear to present practical

(33) Vaska, L.; Diluzio, J. W. *J. Am. Chem. Soc.* **1962**, *84*, 679–680.

(34) Pino, P. *Ann. N.Y. Acad. Sci.* **1983**, *415*, 111–28.

(35) James, B. *Homogeneous Hydrogenation*; Wiley: New York, 1973.

(36) Oro, L.; Sola, E. Mechanistic aspects of dihydrogen activation and catalysis by dinuclear complexes. In *Recent Advances in Hydride Chemistry*; Peruzzini, M., Poli, R., Eds.; Elsevier: Amsterdam, 2001; pp 299–327.

(37) Garland, M.; Pino, P. *Organometallics* **1990**, *9*, 1943–1949.

difficulties to implementation. Finally, there are numerous reasons to assume that hetero-bimetallic CBERs present entirely new opportunities for controlling selectivity. By modifying one or both metals with appropriate ligands, new regio- and possibly stereoselectivity patterns should arise.

Conclusions

Hetero-bimetallic catalytic binuclear elimination (Heck–Breslow II mechanism) exists in the rhodium–rhenium bimetallic hydroformylation of cyclopentene. This is demonstrated by (1) the in situ observation of both mononuclear and hetero-bimetallic intermediates, (2) the synchronized kinetics for the transformation of mononuclear and dinuclear intermediates, (3) the statistical correspondence of both the mononuclear and dinuclear intermediates with product formation, and (4) the rapid hydrogen activation kinetics on $\text{RhRe}(\text{CO})_9$. Moreover, this mechanism is orders of magnitude more efficient than the corresponding unicyclic rhodium catalysis. This finding should promote the search for CBER mechanisms applicable to other types of organic syntheses.

Experimental and Numerical Aspects

The hydroformylations were performed with puriss cyclopentene (99.9% Fluka), carbon monoxide (99.97% Saxol), hydrogen (99.999% Saxol), $\text{Rh}_4(\text{CO})_{12}$ (98% Strem), $\text{HRe}(\text{CO})_5$ (99% Strem), and puriss *n*-hexane (99.6% Fluka). The alkene, gases, and solvent were extensively purified prior to use according to previously used procedures,^{25b} and all solution preparations and transfers were made under Schlenk techniques.³⁹ Triply labeled cyclopentane carboxaldehyde $\text{CH}_2\text{CH}_2\text{CH}_2\text{CHDCH} - ^{13}\text{CDO}$ was made by deuteroformylation of cyclopentene with ^{13}CO using $\text{Rh}_4(\text{CO})_{12}$ as precursor followed by purification.

All hydroformylation experiments were performed in a closed batch reactor system, and mass transfer concerns were addressed (see Supporting Information for details).⁴⁰ The duration of a typical hydroformylation reaction was ca. 5 h, and ca. 15% conversion of cyclopentene was achieved in the standard experiment. Only cyclopentane carboxaldehyde could be detected as product. Mole fractions

are used throughout for kinetic analyses, and all standard deviations are given with 95% confidence levels.

The experimental design for this study is provided in Table 1. Each experiment involved 300 mL of *n*-hexane. The range of concentrations covered by this experimental design was $x_{\text{HRe}(\text{CO})_5} = 1.72 \times 10^{-5} - 1.28 \times 10^{-4}$; $x_{\text{Rh}_4(\text{CO})_{12}} = 5.40 \times 10^{-6} - 4.01 \times 10^{-5}$; $x_{\text{CP}} = 1.49 \times 10^{-2} - 7.40 \times 10^{-2}$; $x_{\text{CO}} = 7.55 \times 10^{-2} - 1.42 \times 10^{-1}$; $x_{\text{H}_2} = 4.90 \times 10^{-3} - 1.91 \times 10^{-2}$; the temperature was $T = 282.6 - 298.5$ K. Blank experiments were performed with cyclopentene, hydrogen, and carbon monoxide as reagents, but without the addition of any organometallic precursors. Monometallic hydroformylation experiments were performed with (i) $\text{HRe}(\text{CO})_5$ as precursor but not $\text{Rh}_4(\text{CO})_{12}$ and (ii) $\text{Rh}_4(\text{CO})_{12}$ as precursor but not $\text{HRe}(\text{CO})_5$. The standard bimetallic hydroformylation experiments were conducted with approximately the average reagent concentrations used in this study. The remaining experiments involved variations in the nominal rhenium and rhodium concentrations, cyclopentene concentrations, partial pressures of the gaseous reactants, and temperature. All 22 bimetallic experiments were started in the same manner by adding in rapid succession $\text{HRe}(\text{CO})_5$ (in *n*-hexane) and then hydrogen to a solution containing cyclopentene and $\text{Rh}_4(\text{CO})_{12}$ under CO. Since both $\text{HRe}(\text{CO})_5$ and hydrogen can be added in ca. 90 s, and since the characteristic time for the disappearance of $\text{Rh}_4(\text{CO})_{12}$ is on the order of 1 h, the sequence of addition plays little role. The general experimental procedure for in situ studies of hydroformylations can be found elsewhere.^{25b}

The FTIR spectra covered the interval 1550–2500 cm^{-1} with data intervals of 0.2 cm^{-1} . The resulting absorbance matrix with dimension 763×4751 was used directly. Band-target entropy minimization²⁷ was used to obtain all pure component spectra, and a set of algebraic system identification algorithms were used to determine the absorptivities of the organic and organometallic species present as well as their moles and mole fractions.⁴¹ The solvent *n*-hexane was used as an internal standard, and its absorptivity was measured independently.

Acknowledgment. The authors would like to thank IBM Singapore and the Institute for High Performance Computing (IHPC Singapore) for the use of the high-performance computational resources used in this study and Dr. Keith J. Carpenter, Director of ICES, for his support.

Supporting Information Available: Detailed signal processing, experimental aspects, and experimental design with mole numbers. This material is available free of charge via the Internet at <http://pubs.acs.org>.

JA073339V

- (38) (a) Chan, Y. Y. Homogeneous Catalytic Binuclear Elimination Reactions in CFSTRs. Application of Feinberg's and Horiuti's Theorems. B. Eng. Thesis, National University of Singapore, 1999. (b) Feinberg, M. In *Mathematical Models of Chemical Reactions*; Erdi, P., Toth, J., Eds.; Manchester University Press: Manchester, 1989; Chapter 4.
- (39) Shriver, D. F.; Drezzdon, M. A. *The Manipulation of Air-Sensitive Compounds*; Wiley: New York, 1986.
- (40) Garland, M. Transport Effects in Homogeneous Catalysis. In *Encyclopedia of Catalysis*; Horvath, I. T., Ed.; Wiley: 2002.

- (41) Widjaja, E.; Li, C.; Garland, M. *J. Catal.* **2004**, 223, 278–289.